Conditionally immortalized human pancreatic stellate cell lines demonstrate enhanced proliferation and migration in response to IGF-I.

Rosendahl, Ann; Gundewar, Chinmay; Said Hilmersson, Katarzyna; Ni, Lan; Saleem, Moin A; Andersson, Roland

Published in:
Experimental Cell Research

DOI:
10.1016/j.yexcr.2014.09.033

2015

Available online at www.sciencedirect.com

ScienceDirect

journal homepage: www.elsevier.com/locate/yexcr

Research Article

Conditionally immortalized human pancreatic stellate cell lines demonstrate enhanced proliferation and migration in response to IGF-I

Ann H. Rosendahl[a,b,*], *Chinmay Gundewar*[a], *Katarzyna Said Hilmersson*[a], *Lan Ni*[c], *Moin A. Saleem*[c], *Roland Andersson*[a]

[a]*Lund University, Department of Clinical Sciences Lund, Division of Surgery, Lund, Sweden*
[b]*Lund University and Skåne University Hospital, Department of Clinical Sciences Lund, Division of Oncology and Pathology, Lund, Sweden*
[c]*University of Bristol, School of Clinical Sciences, Children's Renal Unit and Academic Renal Unit, Bristol, UK*

ARTICLE INFORMATION

Article Chronology:
Received 19 June 2014
Received in revised form
18 September 2014
Accepted 27 September 2014
Available online 7 October 2014

Keywords:
Human pancreatic stellate cells
Conditional immortalization
Temperature-sensitive SV40LT
Pancreatic cancer
IGF

ABSTRACT

Pancreatic stellate cells (PSCs) play a key role in the dense desmoplastic stroma associated with pancreatic ductal adenocarcinoma. Studies on human PSCs have been minimal due to difficulty in maintaining primary PSC in culture. We have generated the first conditionally immortalized human non-tumor (NPSC) and tumor-derived (TPSC) pancreatic stellate cells via transformation with the temperature-sensitive SV40 large T antigen and human telomerase (hTERT). These cells proliferate at 33°C. After transfer to 37°C, the SV40LT is switched off and the cells regain their primary PSC phenotype and growth characteristics. NPSC contained cytoplasmic vitamin A-storing lipid droplets, while both NPSC and TPSC expressed the characteristic markers αSMA, vimentin, desmin and GFAP. Proteome array analysis revealed that of the 55 evaluated proteins, 27 (49%) were upregulated ≥3-fold in TPSC compared to NPSC, including uPA, pentraxin-3, endoglin and endothelin-1. Two insulin-like growth factor binding proteins (IGFBPs) were inversely expressed. Although discordant IGFBP-2 and IGFBP-3 levels, IGF-I was found to stimulate proliferation of both NPSC and TPSC. Both basal and IGF-I stimulated motility was significantly enhanced in TPSC compared to NPSC. In conclusion, these cells provide a unique resource that will facilitate further study of the active stroma compartment associated with pancreatic cancer.

Abbreviations: PSC, pancreatic stellate cell; NPSC, non-tumor derived pancreatic stellate cell; TPSC, tumor-derived pancreatic stellate cell; GFAP, glial fibrillary acidic protein; αSMA, alpha smooth muscle actin; ECM, extra cellular matrix; IGF, insulin-like growth factor; IGFBP, insulin-like growth factor binding protein; ITS, insulin-transferrin-selenium

*Corresponding author at: Lund University and Skåne University Hospital, Department Clinical Sciences Lund, Division of Oncology and Pathology, Barng. 2B, SE-221 85 Lund, Sweden. Fax: +46 46 147327.
E-mail address: ann.rosendahl@med.lu.se (A.H. Rosendahl).

http://dx.doi.org/10.1016/j.yexcr.2014.09.033
0014-4827/

Introduction

Pancreatic ductal adenocarcinoma is a highly malignant tumor with the highest death rate among all cancers. As this cancer shows no symptoms in its early stages it has a low probability of detection, and the majority (>85%) of pancreatic cancer patients already have locally advanced disease or metastases at time of initial diagnosis making them unsuitable for surgical treatment [1]. In addition, pancreatic cancer is resistant to chemotherapy and currently available treatments provide only marginal survival benefits. The characteristic dense stroma surrounding the tumor cells is believed to promote tumor survival and resistance to treatment by creating a physical barrier and block drug distribution [2,3]. Although being a central pathological feature of pancreatic cancer, the cellular and molecular interactions underlying the stroma reaction remain incompletely understood.

Pancreatic stellate cells (PSCs) are myofibroblast-like cells and the key fibrogenic cell type of the pancreas. They are believed to be the source of the stromal reaction associated with pancreatic cancer [4]. PSCs are normally found in an inactive, quiescent state in the healthy pancreas, where they maintain normal pancreatic architecture. Quiescent PSCs can be identified by the presence of cytoplasmic retinoid (vitamin A)-storing lipid droplets and expression of intermediate filaments and mesenchymal markers such as vimentin, desmin and glial fibrillary acidic protein (GFAP) [5,6]. During local inflammation or pancreatic cancer, the PSCs transform from a quiescent to an active state, leading to loss of cytoplasmic vitamin A-storing lipid droplets, increased expression of alpha smooth muscle actin (αSMA) and induction of a number of factors such as PDGF, TGF-β, IL-6 and others that contribute to the aggressive growth of pancreatic cancer [7]. Activated PSCs have also been suggested to play an important role in development of pancreatic cancer metastases by facilitating migration, extracellular matrix (ECM) deposition and remodeling.

Until recently, studies on human PSCs have been minimal due to limited availability of fresh resected pancreatic specimens, as well as difficulties in isolating and culturing these cells in the laboratory environment. Once isolated, the primary PSCs undergo senescence within a limited number of passages, making it difficult to obtain sufficient cell quantities for functional studies [8]. To overcome the limited availability, other laboratories have previously developed immortalized cell lines from human PSCs that unlike the primary cells, divide at a fast rate in the laboratory [9,8]. These cell lines rapidly generate enough cells to study. However, their fast growth rate and continuous proliferation do not accurately represent the primary cell phenotype.

The aim of the present study was to develop exclusively unique and highly relevant cell lines from human normal non-tumor (NPSC) and tumor-derived (TPSC) pancreatic stellate cells. For this purpose, we have generated the first conditionally immortalized human pancreatic stellate cell lines by infection with the temperature-sensitive *SV40LT* gene and telomerase. This technology has been successfully applied previously in cultured human mammary fibroblasts, podocytes, glomerular endothelial and mesangial cells [10–13]. These cells rapidly divide and grow at the "permissive" temperature (33°C). After transfer to the "non-permissive" temperature (37°C), the *SV40LT* gene is switched off and the cells regain their primary PSC phenotype and growth rate. Using these cell lines we sought to identify NPSC and TPSC phenotype characteristics at the protein level and to elucidate their functional responses to insulin-like growth factor-I (IGF-I) on growth and migratory capabilities.

Materials and methods

Primary culture of pancreatic stellate cells

Non-neoplastic and neoplastic pancreatic specimens were obtained from a patient with moderately differentiated pancreatic ductal adenocarcinoma and new onset type-2-diabetes undergoing primary surgical resection. This study was approved by the regional ethical review board in Lund, Sweden. Isolated pancreatic stellate cells from adjacent safe margin specimen were considered to be normal. Pancreatic stellate cells were isolated by the outgrowth method as described previously [6] and cultured in 25-cm^2 flasks in DMEM/Hams Nutrient Mix F12 (Invitrogen, Paisley, UK) medium with added antibiotics (100 U/ml penicillin and 100 μg/ml streptomycin; Invitrogen), 1% Amphotericin-B (Sigma-Aldrich, St. Louis, Mo, USA), 2 mM L-glutamine (Sigma-Aldrich) and 10% FBS (Invitrogen) in a humidified 5% CO_2 atmosphere at 37°C. Pancreatic stellate cell outgrowths appeared at 7–14 d, and allowed to reach 80% confluence before the cells were passaged and transfected with the tsSV40LT gene and hTERT constructs.

Conditional immortalization – retroviral constructs and virus infection

A packaging cell line producing a bicistronic construct containing a temperature-sensitive simian virus-40 large T-antigen (tsSV40LT) and human telomerase (hTERT) as described previously was used [10]. Briefly, cultures of primary human non-tumor or tumor-derived PSCs (at passage 3) were infected with retrovirus-containing supernatants from the packaging cell line (tsTTERT C126). Midconfluent cells in log-phase growth were exposed to freshly thawed filtered (0.45 μm) supernatant mixed 7:3 with growth medium and 10 μg/ml polybrene (Sigma-Aldrich). After 24 h, cultures were replaced with normal growth medium and the cells were allowed to reach confluence at 37°C. The culture medium was then supplemented with 0.5 mg/ml G418 (Life Technologies BRL, Paisley, UK) until selection was completed (14 days). Selection and continuous culture were carried out at 33°C. After 2 weeks clones of healthy selected cells began to appear. Surviving cells were allowed to approach confluence in standard medium. Subcloning by limited dilution was achieved by seeding cells in 96-well plates at a density of ~1 cell/well. Approximately 10 clones of each cell line were further characterized based on the greatest similarity to the primary cells and subjected to a second round of subcloning and characterization. Conditionally immortalized PSCs were growth in RPMI 1640 medium supplemented with antibiotics (100 U/ml penicillin and 100 μg/ml streptomycin; Invitrogen), ITS (Sigma-Aldrich) and 10% FBS (GIBCO). Cells were grown to 80% confluence before thermo-switching to 37°C. At both temperatures, cells were fed with fresh medium three times per week.

Martius scarlet blue staining

Biopsies of residual tissues used for PSC isolation were fixed, paraffin embedded, sectioned 4 μm and routinely processed for Martius scarlet blue staining (MSB). Collagen and connective tissue are visualized in blue, while fibrin and zymogen granules are stained in bright red.

Oil Red-O staining

Cells were cultured (3×10^4 cells/well) in four-well chamber slides (Lab-Tek II Chamber Slide System, Nunc), fixed in 2% paraformaldehyde followed by Oil Red-O staining for cytoplasmic vitamin A storing lipid droplets. Intracellular lipid droplets were examined by light microscopy using a Nikon Eclipse 80i microscope with Nikon DS-Qi1 camera and NIS-Elements software.

Immunofluorescence

Cells cultured (10×10^3 cells/well) in eight-well chamber slides (Lab-Tek II Chamber Slide System, Nunc) were fixed in 2% paraformaldehyde, permeabilized in 1% Triton X-100, blocked (5% donkey serum and 1% Triton X-100) followed by immunofluorescent staining for α-SMA, vimentin, desmin and GFAP at 4°C overnight. Following washing, secondary antibodies (Invitrogen) donkey-anti-goat (Alexa fluor 488) or donkey-anti-mouse (Alexa fluor 488) were added for 1 h at room temperature and nuclei/DNA counterstained with DAPI. Positive staining was analyzed using a Nikon Eclipse 80i microscope with a Nikon DS-Qi1 camera and NIS-Elements software.

Western immunoblotting

Cells were lysed and processed as described previously [14]. Lysates were loaded according to protein concentration, separated (65 μg protein per lane) by SDS-PAGE (12%) and transferred to 0.2 μm Hybond-C extra nitrocellulose membrane (Amersham Biosciences). The blocked membranes were probed overnight (4°C) with the following antibodies: anti-SV40LT (BD Pharmingen PAb101; 1:1000), anti-vimentin (R&D Systems AF2105; 1:500), anti-α-SMA (DAKO M0851; 1:2000), anti-desmin (R&D Systems AF3844; 1:500), anti-GFAP (SigmaAldrich G-A-5; 1:1000) and anti-GAPDH (Millipore MAB374; 1:1000). Subsequently, the membranes were incubated with horseradish peroxidase (HRP)-conjugated secondary antibody and visualized by SuperSignal West Dura Substrate (PIERCE, ThermoScientific) using LI-COR Odyssey Fc imaging system and Image Studio software (LI-COR Biosciences Ltd, Cambridge, UK).

Cell cycle analysis

Primary or conditionally immortalized NPSC and TPSC were seeded in flasks at subconfluent density, placed at either 33°C or 37°C. Cells were harvested, fixed in ice cold 70% ethanol, stained with PI/RNAse buffer (BD Biosciences, San Diego, CA), and subjected to cell cycle analysis (FL2-A) on a FACSCalibur flow cytometer (BD Biosciences) with CellQuest Pro software (BD Biosciences). Approximately 2×10^5 events (cells) were evaluated for each sample using FlowJo Vx software (Tree Star Inc, Ashland, OR, USA).

Proteome profiler array

Proteins were extracted from cultured NPSC and TPSC and concentration determined as above. Equal amounts of protein were evaluated using the Proteome Profiler™ Human Angiogenesis Array, according to the manufacturer's instructions (R&D Systems) and visualized by SuperSignal West Dura Substrate (PIERCE, ThermoFisherScientific) using the LI-COR Odyssey Fc imaging system and Image Studio software (LI-COR Biosciences Ltd, Cambridge, UK). Relative levels of protein expression were quantified by analyzing the average pixel density after background correction. Heat map of fold difference in relative protein abundance was generated by comparing the pixel densities (normalized to internal assay controls) of the corresponding signals between NPSC and TPSC at 37°C.

Cell proliferation

Cells were seeded (10×10^3 cell/well) in 96-well plates in growth media for 24 h before switching to serum-free media (SFM) for a further 24 h. Cells were subsequently dosed with IGF-I (100 ng/ml) in SFM in quadruplicate ($n=4$ wells). Following incubation for 24 h, the cell proliferation was assessed by tetrazolium dye [3-(4,5-dimethylthiazol-2-yl)-2,5-diphenyltetrazolium-bromide] (MTT; Cell Proliferation Kit I) assay according to the manufacturer's instructions (R&D Systems). The samples were measured on a Labsystems Multiskan Plus plate reader (test wavelength 595 nm, reference wavelength 660 nm) using the DeltaSoft JV software (BioMetallics Inc., Princeton, NJ, USA). Cell proliferation in the time-course experiments of SV40LT silencing after thermoswitching was determined by cell counting using trypan blue dye exclusion.

Invasion and motility assays

The invasion assay was performed using Transwell cell culture inserts (24 wells, 8-μm pore size; BD Biosciences). Briefly, 5×10^4 NPSC or TPSC cells in 300 μl SFM were added to the culture inserts upper chamber. SFM with or without IGF-I (100 ng/ml) was added to the lower chamber. After 24 h, the non-invading cells on the upper surface of the insert membrane were removed using cotton swabs. Invaded cells were fixed in 1% glutaraldehyde, stained with 0.5% crystal violet for 30 min and counted at 10× magnification in four different microscopic fields for each insert. The experiments were repeated at least three times. Additionally, TPSC motility was assayed using scratch assay. TPSCs were seeded at confluence in four-well chamber slides in growth media for 24 h before switching to SFM for a further 24 h. Wounds were made using sterile white pipette tips prior to dosing as above. Following 16 h migration, the cells were fixed in 2% paraformaldehyde, permeabilized in 1% Triton X-100 and exposed to Alexa Fluor 488-conjugated phalloidin (Life Technologies) and DAPI to visualize F-actin cytoskeleton and nuclei, respectively.

Statistical analysis

The data were presented as means ± SE. Statistical analyses were performed using two-tailed Student's t-test. A P-value of <0.05 was considered statistically significant.

Results

Cell culture and vitamin A-storing lipid droplet abundance

Primary human PSCs were isolated from residual normal and pancreatic cancer surgical specimens. MSB staining of the tissues verified a normal pancreatic histology and a moderately differentiated tumor with highly abundant stroma in blue (Fig. 1A). Conditionally immortalized human non-tumor (NPSC) and tumor-derived (TPSC) pancreatic stellate cell lines were developed by restoring functional telomerase activity and introducing the temperature-sensitive *SV40T* gene. These cells demonstrated enhanced proliferation at the permissive temperature 33°C, while after transfer to the nonpermissive temperature 37°C they regained a low proliferation rate. PSCs were used in experiments after at least 6 days at 37°C. The PSCs were validated for the presence of cytoplasmic vitamin A-containing lipid droplets. Primary NPSC displayed multiple cytoplasmic lipid droplets, characteristic of a quiescent state (Fig. 1B). Actively proliferating conditionally immortalized NPSCs had reduced cell bodies with less lipid droplets. Post-thermoswitching, the morphology and lipid droplet abundance appeared similar to the primary parental cells indicating a quiescent NPSC phenotype. In contrast, both primary and conditionally immortalized TPSCs displayed significantly less cytoplasmic lipid droplets indicative of an active state (Fig. 1B).

Verifying the expression of PSC markers in cultured PSCs

In culture, PSCs resemble activated myofibroblasts, expressing a variety of mesenchymal and myofibroblast-associated proteins. To confirm the phenotype of the conditionally immortalized NPSC and TPSC, a combination of characteristic cell markers were examined by immunofluorescence and Western blot. The intermediate filament and general mesenchymal marker vimentin, as well as the principle actin isoform associated with myofibroblasts α-SMA, were strongly expressed in a linear pattern in the cytoplasm of both NPSC and TPSC (Fig. 2A). Additional intermediate filaments, desmin and glial fibrillary acidic protein (GFAP) were also expressed in PSCs. The immunostaining results were supported by Western blot confirming the expression of PSC cell markers α-SMA, vimentin, desmin and GFAP (Fig. 2B). Densitometry quantification revealed higher α-SMA, vimentin and desmin abundance post-thermoswitching compared to the actively proliferating state at 33°C (Fig. 2B).

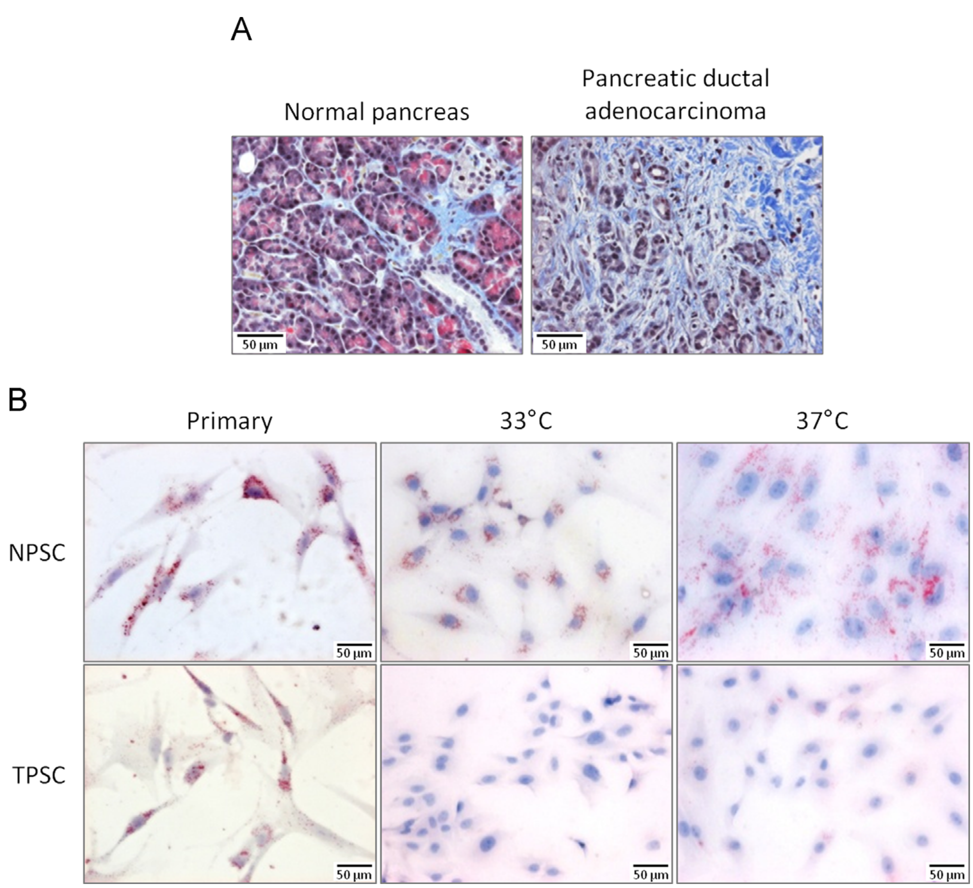

Fig. 1 – Morphology and activation status of cultured NPSC and TPSC at 33°C and 37°C. (A) Martius scarlet blue staining of normal pancreatic tissue and pancreatic ductal adenocarcinoma with massive stroma in blue. (B) Oil Red-O staining of vitamin-A storing lipid droplets of primary and conditionally immortalized NPSC and TPSC at 33°C and after 7 days at 37°C. Images demonstrating a high abundance of characteristic lipid droplets in primary and immortalized NPSC indicative of a quiescent phenotype. The weak cytoplasmic expression of lipid droplets in primary and immortalized TPSC, indicate a more active phenotype. Scale bars = 50 µm.

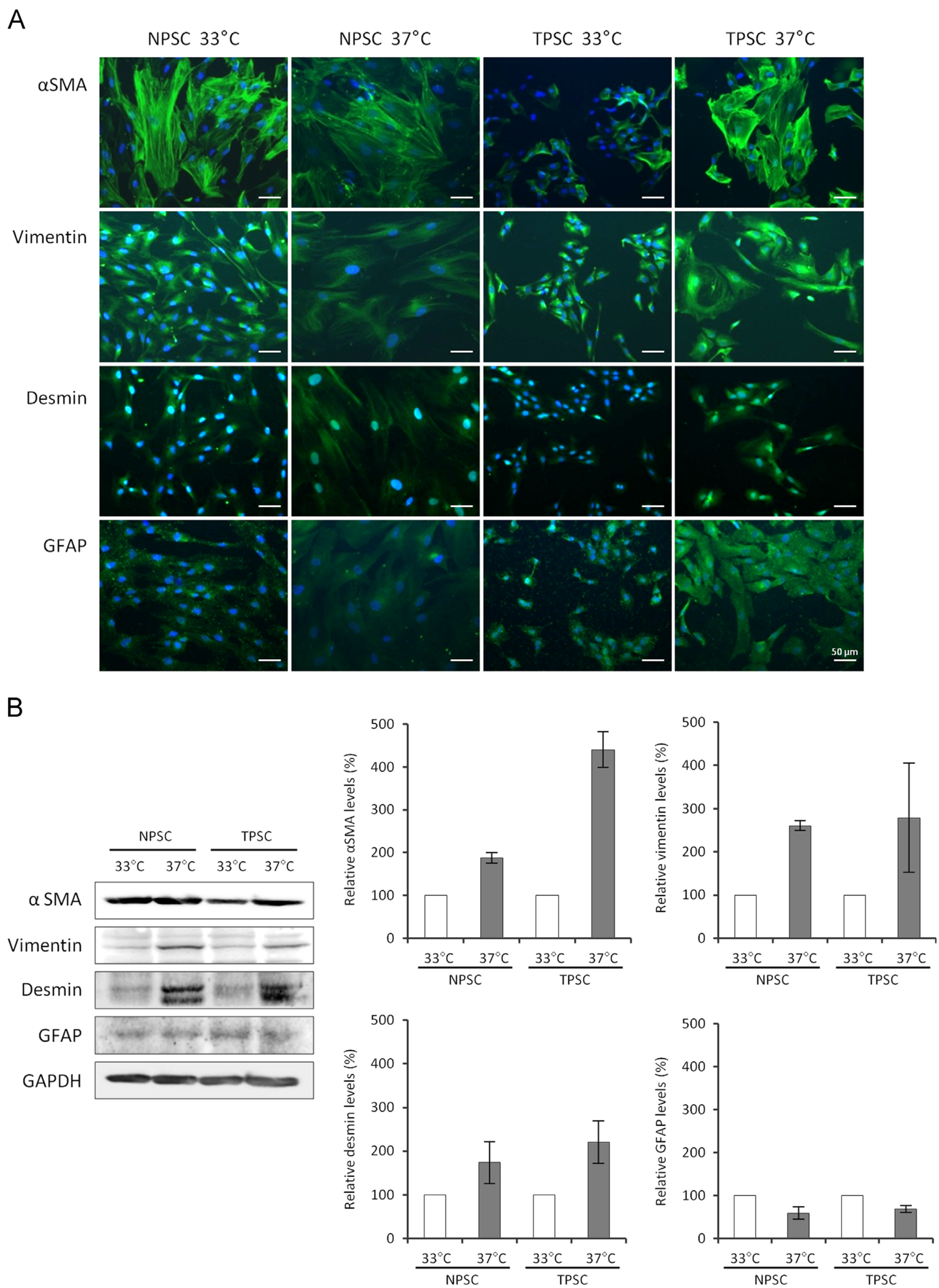

Fig. 2 – Expression of characteristic pancreatic stellate cell markers in conditionally immortalized NPSC and TPSC at 33°C and after 7 days at 37°C. (A) Immunofluorescent staining of αSMA, vimentin, desmin and GFAP. Scale bars = 50 μm. (B) Western blotting analyses confirming the expression of pancreatic stellate cell specific markers. GAPDH is shown as a loading control. One representative blot of three independent experiments is shown. Relative protein abundance was quantified by densitometry analysis and corrected for GAPDH. The graphs show modulation of relative protein abundance at 37°C versus 33°C and represent the mean ± SE.

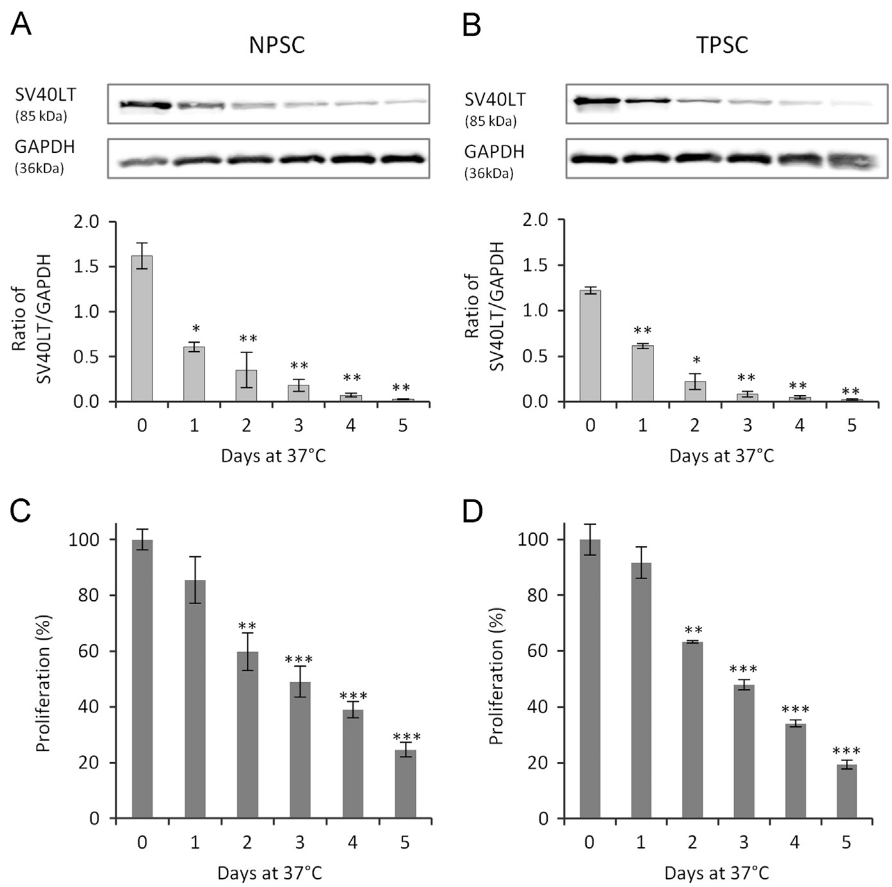

Fig. 3 – Silencing of tsSV40LT after thermoswitching of NPSC and TPSC. Time-course analysis of tsSV40LT protein expression in (A) NPSC and (B) TPSC at 33°C (day 0) and at 37°C (days 1–5). Western immunoblot and densitometry analysis shows a rapid decline in SV40LT expression after the transfer to nonpermissive temperature 37°C. GAPDH was used as a loading control. Cell proliferation analyzed by cell counting showed a significant declining growth rate of (C) NPSC and (D) TPSC after thermoswitching to 37°C. Data is shown as percent growth compared to control cells at 33°C. Graphs represent mean ± SE of three independent experiments. $^{*}P<0.05$, $^{**}P<0.01$, $^{***}P<0.001$.

SV40LT silencing after thermoswitching

Western blotting confirmed the successful transformation and expression of SV40LT in both NPSC (Fig. 3A) and TPSC (Fig. 3B) at 33°C where the antigen is active and allowing enhanced cell proliferation. Time-course analysis showed a rapid silencing of the tsSV40LT antigen after thermoswitching the cells to 37°C (Fig. 3A,B). The SV40LT silencing was reflected in the reduced growth rate observed over time in both NPSC (Fig. 3C) and TPSC (Fig. 3D).

Cell cycle distribution

Cell cycle distribution was compared between primary TPSC and conditionally immortalized NPSC and TPSC grown at 33°C and 37°C. Insufficient cell quantities prohibited cell cycle analysis of primary NPSCs. Primary TPSCs showed a very low level of proliferation with more than 80% of the cells in G_0/G_1 phase, while only 3.4% were found in DNA synthesis (S-) phase and 6.8% growing and actively dividing in G_2/M phase (Fig. 4A,B). Conditionally immortalized TPSCs grown at the permissive temperature 33°C proliferated rapidly with approximately 10% in S-phase and 21% in G_2/M phase, while only 68% were in G_0/G_1 phase. Importantly, after 5 days at 37°C and the tsSV40LT switched off, the conditionally immortalized TPSCs demonstrated high resemblance to primary TPSCs, with a detectable, but low level of proliferation. A similar cell cycle distribution was observed for NPSC when grown under these conditions (Fig. 4A,B).

Proteome profiler array

To further characterize the conditionally immortalized PSCs, a panel of 55 different proteins was evaluated by proteome profiler array comparing NPSC and TPSC at both the permissive and non-permissive temperatures. Overall the expression patterns were similar between the permissive and non-permissive temperatures, in both NPSC and TPSC (Fig. 5A). However, several differences in the expression pattern were observed between NPSC and TPSC (Fig. 5B). Among the 55 evaluated proteins, 37 were upregulated ≥2-fold, and 27 were upregulated ≥3-fold in TPSC compared to NPSC. In contrast, only 4 proteins were upregulated ≥2-fold in NPSC compared to TPSC. Several proteins involved in angiogenesis regulation and matrix remodeling (tissue factor, thrombospondin-1, plasminogen activator inhibitor-1, tissue inhibitor of matrix metalloproteinases-1, fibroblast growth factor-1 and -2) were among the abundantly expressed proteins. Among the top differentially expressed and elevated proteins in TPSC were urokinase plasminogen activator (uPA, $P=0.033$), pentraxin 3 (PTX3, $P=0.0047$),

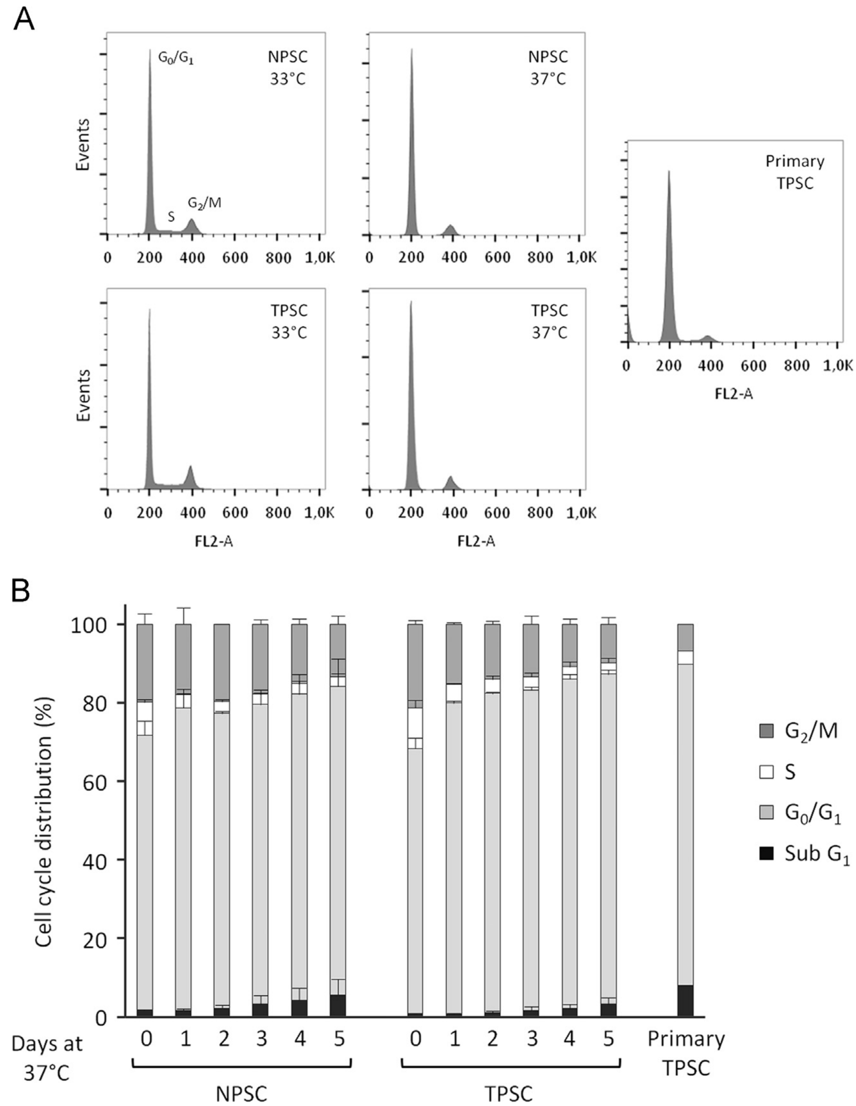

Fig. 4 – Cell cycle distribution of primary TPSC and conditionally immortalized NPSC and TPSC. (A) Cell cycle histograms of conditionally immortalized NPSC and TPSC at the growth-permissive (33°C) and non-permissive (37°C, 5 days) temperatures, relative to primary TPSC. (B) Flow cytometry evaluation of cell cycle distribution (%) of conditionally immortalized NPSC and TPSCs at 33°C (day 0) and at 37°C (days 1–5) versus primary TPSCs. Data is shown as mean+SE of three individual repeats for conditionally immortalized NPSC and TPSC, and for one repeat of primary TPSC due to the limited availability of primary cells.

insulin-like growth factor binding protein 2 (IGFBP-2, $P=0.012$), endoglin ($P=0.055$) and endothelin-1 ($P=0.026$). In contrast, IL-1β ($P=0.024$) and CCL-2 (MCP-1, $P=0.029$) were reduced in TPSC compared to NPSC. Interestingly, the two IGFBPs -2 and -3 were inversely expressed with IGFBP-2 predominantly expressed in TPSC (6.6-fold enhanced, $P=0.012$), while IGFBP-3 was primarily expressed in NPSC (6.7-fold enhanced, $P=0.0048$).

IGF-I stimulates proliferation and motility of pancreatic stellate cells.

Following the observation that the IGFBP-2 and IGFBP-3 were inversely expressed in NPSCs and TPSC, we evaluated the responsiveness to IGF-I stimulation on PSC proliferation and migration. Exposure to IGF-I for 24 h increased the proliferation of NPSC by 33% ($P<0.01$) and TPSC by 50% ($P<0.001$) compared with controls (Fig. 6A). IGF-I also increased PSC motility and invasion, as measured by scratch and Transwell assays (Fig. 6B–D). The presence of IGF-I enhanced TPSC invasion by 3.6-fold ($P<0.001$) compared to basal, while enhancing NPSC invasion by 2.6-fold ($P<0.01$). Notably, TPSC showed a significantly increased basal (9.2-fold, $P<0.001$) and IGF-I-stimulated (12.4-fold, $P<0.001$) motility compared to NPSC (Fig. 6B, C). The TPSC motility displayed an organized, ray-like pattern with all migrating TPSCs demonstrating a dense lamellipodium network with protrusions at the leading edge, as visualized by phalloidin staining of F-actin cytoskeleton in a scratch assay (Figs. 6D,E). These results demonstrate that both basal and IGF-I-stimulated motility of TPSC were significantly enhanced compared to NPSC.

Discussion

Pancreatic cancer is associated with a highly abundant stroma. The tumor microenvironment and pancreatic stellate cells in particular are recognized to play a major role in the aggressiveness of this disease. However, previously studies on pancreatic stellate cells have been minimal due to difficulty of maintaining primary human pancreatic stellate cells in culture for a long time, thus limiting experiments with sufficient replicates. Our study is the first to report the generation of conditionally immortalized human non-tumor and tumor-derived pancreatic stellate cell lines. These cells will provide a highly significant and unique resource for further study of human PSCs and their role in pancreatic cancer progression, local inflammation and response to treatments.

Other laboratories have established human pancreatic stellate cell lines immortalized with SV40LT, which continuously proliferate and can be grown for prolonged time [9,8]. However, previously established PSC lines have been generated without the ability to switch off SV40LT. The use of a temperature-sensitive SV40LT allows unlimited replication at the permissive temperature, while transfer to the non-permissive temperature 37°C switches off SV40 allowing the cells to regain their native characteristics with minimal interference with the primary cell phenotype. As primary stellate cells grow slowly, the conditional immortalization will provide a highly relevant and representative cell model.

Actively proliferating conditionally immortalized NPSCs and TPSCs displayed reduced cell bodies at the growth permissive temperature. In contrast, post-thermoswiching, the morphology appearance was different and the cells regained a larger stellate cell shape, similar to the primary parental PSCs. This change in morphology is consistent with a reduced growth rate of cultured PSCs and a shift toward the G_1 phase of the cell cycle [15]. The conditionally immortalized cells expressed high levels of tsSV40LT at the growth-permissive temperature allowing them to proliferate. However, the SV40LT levels were rapidly reduced following transfer of the cells to the non-permissive temperature. After 5 days at 37°C, the immortalized stellate cells showed equivalent cell cycle distribution and phenotypic characteristics of primary stellate cells in culture. Both NPSC and TPSC were positive for the characteristic markers vimentin, desmin, GFAP and αSMA. Notably, the NPSCs had considerably higher levels of cytoplasmic lipid droplets compared to TPSCs. Vitamin A-storing lipid droplets are associated with a quiescent state of PSCs and are described as one of the major distinguishing features between normal resident PSCs and activated tumor-associated PSCs [16].

To further establish the phenotype of the immortalized cells we compared the protein profiles between NPSC and TPSCs. PSCs play important roles in the local tumor microenvironment by regulating ECM composition and negatively influence angiogenesis [17]. Indeed, we found the PSCs to express several novel as well as previously reported proteins involved in matrix remodeling (urokinase plasminogen activator; uPA, matrix metalloproteinases; MMPs, and plasminogen activator inhibitor-1; PAI-1) and suppressing angiogenesis (endostatin, angiostatin and thrombospondin). Among the 55 evaluated proteins, 37 were upregulated

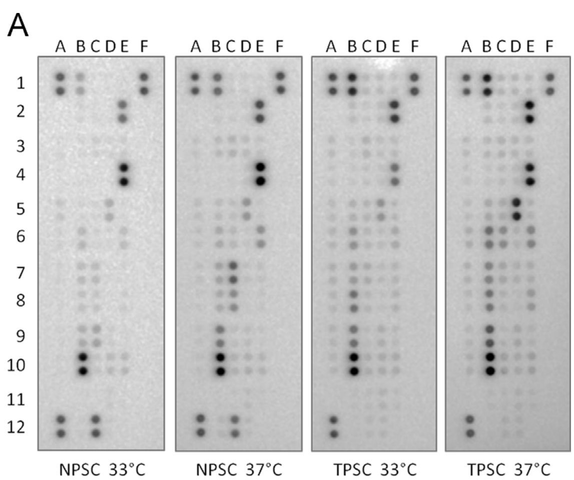

B

	NPSC	TPSC
* uPA	0,020	0,244
** Pentraxin 3(PTX3)	0,268	2,027
* IGFBP-2	0,057	0,379
(*) Endoglin (CD105)	0,120	0,738
* GDNF	0,013	0,078
* Endothelin-1 (ET-1)	0,104	0,625
* Serpin B5	0,011	0,063
EGF	0,006	0,035
* FGF-4	0,006	0,027
* MIP-1alpha	0,016	0,072
* Leptin	0,006	0,028
* Vasohibin	0,013	0,056
* CXCL16	0,018	0,071
Angiostatin/Plasminogen	0,013	0,050
HGF	0,012	0,047
TIMP-4	0,014	0,051
* PDGF-AB/PDGF-BB	0,007	0,026
Artemin	0,021	0,074
ADAMTS-1	0,009	0,033
* Persephin	0,038	0,126
* PDGF-AA	0,025	0,083
* PD-ECGF	0,017	0,056
* Angiopoietin-1	0,033	0,103
** Thrombospondin-2	0,030	0,093
MMP-8	0,022	0,067
* EG-VEGF	0,046	0,139
** Endostatin (Collagen XVIII)	0,157	0,476
** VEGF-C	0,012	0,035
LAP(TGF-B1)	0,060	0,177
IGFBP-1	0,032	0,094
* VEGF	0,064	0,169
* Tissue Factor	0,750	1,948
* Angiopoietin-2	0,032	0,084
Amphiregulin	0,022	0,054
Serpin F1	0,030	0,071
* FGF acidic (FGF-1)	0,541	1,197
* Activin A	0,024	0,051
PIGF	0,028	0,061
Prolactin	0,031	0,061
* PAI-1 (Serpin E1)	1,197	2,327
GM-CSF	0,016	0,030
** Thrombospondin-1	0,313	0,481
* MMP-9	0,053	0,079
NRG1-B1	0,041	0,059
* FGF basic (FGF-2)	2,556	3,656
DPPIV	0,050	0,066
HB-EGF	0,079	0,093
* Platelet factor 4(PF4)	0,086	0,101
Angiogenin	0,042	0,046
IL-8	0,030	0,026
** TIMP-1	3,194	2,249
FGF-7	0,036	0,015
* IL-1β	0,327	0,054
** IGFBP-3	0,852	0,128
* CCL2 (MCP-1)	0,721	0,070

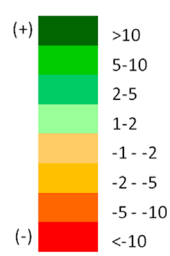

Fig. 5 – Protein expression by proteome profiler array of NPSC and TPSC. (A) The protein expression patterns were similar between the permissive (33°C) and non-permissive (37°C) temperatures, in both NPSC and TPSC. (B) Relative levels of the analyzed proteins, quantified by densitometry and shown in a heat map to illustrate differential levels between NPSC and TPSC at 37°C. Colored bar indicate fold difference (green, enhanced; red, reduced) between TPSC and NPSC protein levels ($n=2$). $^{(*)}P=0.055$, $^{*}P<0.05$, $^{**}P<0.01$.

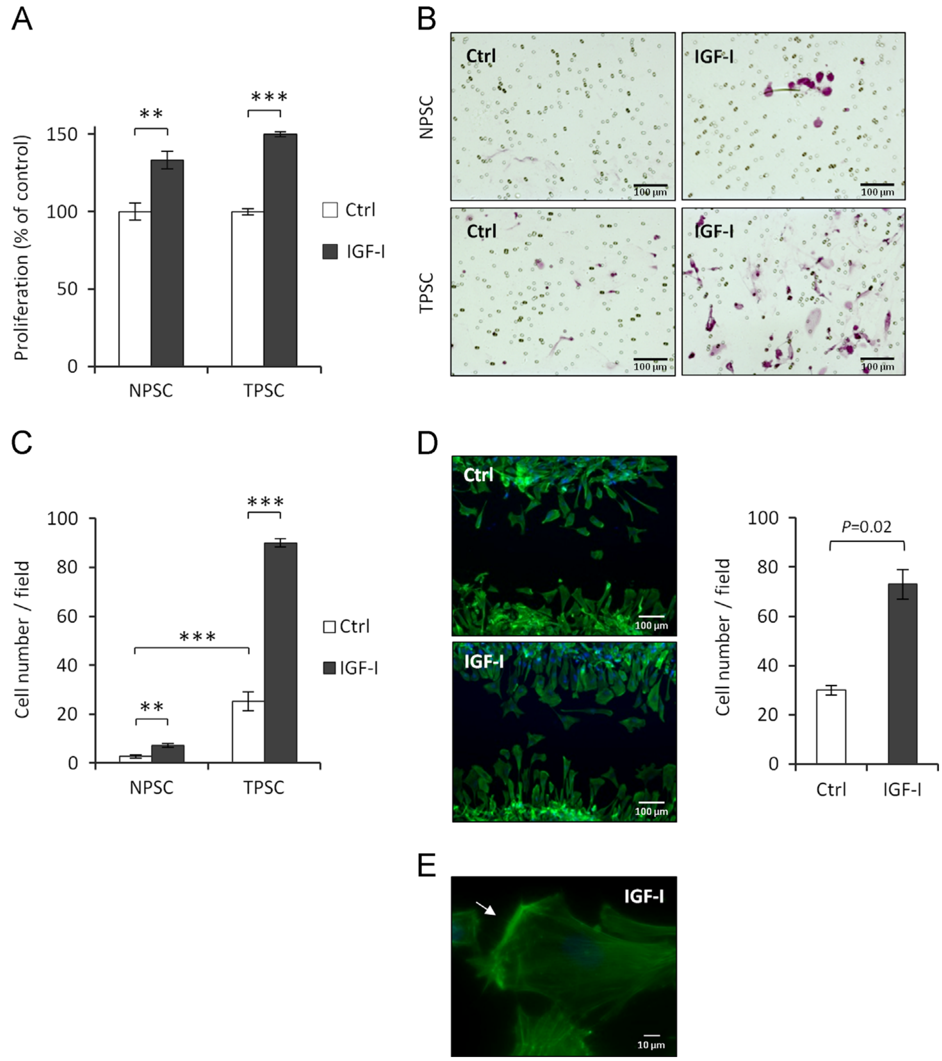

Fig. 6 – Pancreatic stellate cell responsiveness to growth factors. (A) NPSC and TPSC were exposed to IGF-I (100 ng/ml) for 24 h and cell proliferation analyzed by MTT. Data represent mean ± SE of four replicate wells from one out of three individual experiments. (B, C) Invasive capabilities of NPSC and TPSC after 24 h transwell invasion with IGF-I (100 ng/ml) or SFM control added to the lower chamber. (B) Representative images from one of three independent experiments are shown. Scale bars = 100 µm. (C) Graph represents number of invaded cells as mean ± SE in four fields for each insert (magnification 10 ×). Both basal and IGF-I-induced invasion was significantly higher in TPSC compared to NPSC. (D) Basal and IGF-I-stimulated motility of TPSC after 16 h migration in a scratch assay. Scale bars = 100 µm. (D, E) F-actin cytoskeleton is visualized in green and nuclei by DAPI staining in blue. (E) White arrow indicates the dense lamellipodium network with protrusions at the leading edge of IGF-I stimulated TPSC. Scale bar = 10 µm. $^{**}P<0.01$, $^{***}P<0.001$, Student's *t*-test.

≥ 2-fold in TPSC compared to NPSC. uPA was the most upregulated protein and 12-fold enhanced in TPSC compared to NPSC. uPA is known to modulate cell adhesion and enhance both cell proliferation and migration of many tumors. Amplification of the uPA receptor gene, thus rendering tumors more sensitive to uPA, has been implicated in pancreatic cancer progression [18].

The membrane glycoprotein endoglin and the vasoconstricting peptide endothelin-1 were also among the top differently expressed proteins, both enhanced > 6-fold in TPSC relative to NPSC. Endoglin is part of the TGF-β receptor complex and modulates TGF-β responses [19]. The enhanced endoglin expression by TPSC may contribute to increased responsiveness to profibrotic stimuli by TGF-β and thus promote the excessive fibrotic process in the pancreatic tumor stroma, as previously shown for murine hepatic stellate cells [20]. Furthermore, endoglin contains an RGD-sequence that enables cell adhesion via interaction with integrin receptors and ECM components such as fibronectin [21]. Endothelin-1 has previously been reported to be expressed by primary rat PSC and to stimulate their contraction and migration [22]. The elevated levels of endoglin and endothelin-1 by TPSC may thus contribute to the more motile cell phenotype compared to NPSC.

In addition to their matrix and angiogenesis regulating roles, the tumor-associated PSCs are implied to amplify the local and systemic low-grade inflammation associated with pancreatic cancer. Most interestingly, we found the inflammatory response mediator pentraxin 3 (PTX3), closely related to C-reactive protein (CRP), to be almost 8-fold upregulated in TPSC versus NPSC.

Recently, a direct relationship between PTX3 levels, pancreatic cancer migratory activity, and patient prognosis was reported [23]. Pancreatic cancer patients with high PTX3 levels had both significantly shorter progression free survival and shorter overall survival compared to patients with low PTX3 levels. In addition, it was suggested that PTX3 may be used as a promising biomarker in pancreatic cancer prognosis. However, the biological and clinical relevance of TPSC-derived PTX3 as well as the matrix and angiogenesis regulating factors reported herein on tumor progression, remains to be elucidated.

Although genetic differences were not evaluated within the present study, previous genome-wide profiling have identified disease specific transcriptional fingerprints between normal-, pancreatitis- and pancreatic cancer-associated PSCs [24,25]. Together with the current profiling data reported herein, these findings suggest that stellate cells of different activation stages may acquire genetic or cellular adaptations which appear sustained and influence their phenotype characteristics.

Interestingly, two insulin-like growth factor binding proteins (IGFBP) were inversely expressed in NPSC and TPSC. IGFBP-2 was $>$6-fold more abundant, while IGFBP-3 was equally less abundant in TPSC compared to NPSC. IGFBP-2 and IGFBP-3 are two major regulators of the stability and bioavailability of IGF-I, a potent mitogen for numerous tumor types including pancreatic cancer [26,27]. High levels of IGF-I with concurrently low levels of IGFBP-3 has been associated with increased risk of pancreatic cancer [28]. IGFBP-2 can promote a maintained activation status of the mitogenic IGF/PI3K pathway by negatively regulate PTEN abundance [29]. The discordant IGFBP-2 and IGFBP-3 levels in TPSC may thus in a paracrine fashion be involved in enhancing pancreatic cancer cell growth by stabilizing IGF-I levels in the local tumor area as well as enhancing the activity of IGF/PI3K pathway. IGF-I has been demonstrated as an important mitogen for liver myofibroblasts [30]. IGF-I is also known to stimulate both pancreatic cancer cell proliferation and motility [31]. Yet, to our knowledge no studies of direct effects of IGF-I on human PSC have been reported. Although an inverse expression of IGFBP-2 and IGFBP-3, IGF-I was found in the present study to stimulate proliferation of both NPSC and TPSC. In addition, our data indicate for the first time that the invasive capabilities of PSCs increased in response to IGF-I. Interestingly, the IGF-I-stimulated motility was significantly higher in TPSC compared to NPSC. Recently, TPSCs were shown to co-migrate with pancreatic cancer cells from the primary site to the metastatic lesions, where they create a growth permissive environment [32]. As IGF-I often is overexpressed by tumor cells, this may contribute to facilitate PSC motility in a paracrine fashion and thus influence the aggressiveness of the disease [33]. In addition, it is plausible that the PSC-derived IGFBPs may influence the tumor cells and PSCs both in an IGF-dependent and independent manner in the local tumor microenvironment [29,34].

A potential limitation of this study, as with many unique cell lines, may be that the conditionally immortalized TPSC and NPSC reported herein are generated from one individual. For future perspectives it would be highly valuable to generate additional PSC cell lines using the same temperature-sensitive conditionally immortalization approach. With the well-known pancreatic tumor heterogeneity, a broader panel of PSC cell lines would allow for the comparison of inter-individual variations in PSC cellular characteristics within a patient population, and provide the means of a more generalized understanding of their impact on tumor behavior.

In summary, our study is the first to report the generation of conditionally immortalized human non-tumor and tumor-derived pancreatic stellate cell lines, which will be important in studies of the active stroma compartment associated with pancreatic cancer. The discordant expression of the identified matrix-, angiogenesis-, inflammatory- and growth regulating factors by TPSC and NPSC may potentially be of clinical relevance and warrant further investigation. A better understanding of the active stroma compartment is significant to the identification of novel therapeutic opportunities and improved patient outcome.

Acknowledgments

We thank Prof. Parmjit Jat (University College London, UK) and the Ludwig Institute for Cancer Research (NY, USA) for generously providing the tsSV40LT and human telomerase (hTERT) retroviral construct. This study was supported in part by the Royal Physiographic Society Lund, the Gyllenstiernska Krapperups' foundation and the John and Augusta Persson foundation. The authors declare no conflicts of interest.

REFERENCES

[1] M. Hidalgo, Pancreatic cancer, N. Engl. J. Med. 362 (2010) 1605–1617.
[2] R. Kadaba, H. Birke, J. Wang, S. Hooper, C.D. Andl, F. Di Maggio, E. Soylu, M. Ghallab, D. Bor, F.E. Froeling, S. Bhattacharya, A.K. Rustgi, E. Sahai, C. Chelala, P. Sasieni, H.M. Kocher, Imbalance of desmoplastic stromal cell numbers drives aggressive cancer processes, J. Pathol. 230 (2013) 107–117.
[3] K.P. Olive, M.A. Jacobetz, C.J. Davidson, A. Gopinathan, D. McIntyre, D. Honess, B. Madhu, M.A. Goldgraben, M.E. Caldwell, D. Allard, K.K. Frese, G. Denicola, C. Feig, C. Combs, S.P. Winter, H. Ireland-Zecchini, S. Reichelt, W.J. Howat, A. Chang, M. Dhara, L. Wang, F. Ruckert, R. Grutzmann, C. Pilarsky, K. Izeradjene, S.R. Hingorani, P. Huang, S.E. Davies, W. Plunkett, M. Egorin, R.H. Hruban, N. Whitebread, K. McGovern, J. Adams, C. Iacobuzio-Donahue, J. Griffiths, D.A. Tuveson, Inhibition of Hedgehog signaling enhances delivery of chemotherapy in a mouse model of pancreatic cancer, Science 324 (2009) 1457–1461.
[4] M. Erkan, C.W. Michalski, S. Rieder, C. Reiser-Erkan, I. Abiatari, A. Kolb, N.A. Giese, I. Esposito, H. Friess, J. Kleeff, The activated stroma index is a novel and independent prognostic marker in pancreatic ductal adenocarcinoma, Clin. Gastroenterol. Hepatol. 6 (2008) 1155–1161.
[5] M.V. Apte, P.S. Haber, T.L. Applegate, I.D. Norton, G.W. McCaughan, M.A. Korsten, R.C. Pirola, J.S. Wilson, Periacinar stellate shaped cells in rat pancreas: identification, isolation, and culture, Gut 43 (1998) 128–133.
[6] M.G. Bachem, E. Schneider, H. Gross, H. Weidenbach, R.M. Schmid, A. Menke, M. Siech, H. Beger, A. Grunert, G. Adler, Identification, culture, and characterization of pancreatic stellate cells in rats and humans, Gastroenterology 115 (1998) 421–432.
[7] M.B. Omary, A. Lugea, A.W. Lowe, S.J. Pandol, The pancreatic stellate cell: a star on the rise in pancreatic diseases, J. Clin. Invest. 117 (2007) 50–59.
[8] R. Jesnowski, D. Furst, J. Ringel, Y. Chen, A. Schrodel, J. Kleeff, A. Kolb, W.D. Schareck, M. Lohr, Immortalization of pancreatic stellate cells as an in vitro model of pancreatic fibrosis: deactivation is induced by matrigel and N-acetylcysteine, Lab Invest. 85 (2005) 1276–1291.

[9] R.F. Hwang, T. Moore, T. Arumugam, V. Ramachandran, K.D. Amos, A. Rivera, B. Ji, D.B. Evans, C.D. Logsdon, Cancer-associated stromal fibroblasts promote pancreatic tumor progression, Cancer Res. 68 (2008) 918–926.
[10] M.J. O'Hare, J. Bond, C. Clarke, Y. Takeuchi, A.J. Atherton, C. Berry, J. Moody, A.R. Silver, D.C. Davies, A.E. Alsop, A.M. Neville, P.S. Jat, Conditional immortalization of freshly isolated human mammary fibroblasts and endothelial cells, Proc. Natl. Acad. Sci. USA 98 (2001) 646–651.
[11] M.A. Saleem, M.J. O'Hare, J. Reiser, R.J. Coward, C.D. Inward, T. Farren, C.Y. Xing, L. Ni, P.W. Mathieson, P. Mundel, A conditionally immortalized human podocyte cell line demonstrating nephrin and podocin expression, J. Am. Soc. Nephrol. 13 (2002) 630–638.
[12] R.M. Sarrab, R. Lennon, L. Ni, M.D. Wherlock, G.I. Welsh, M.A. Saleem, Establishment of conditionally immortalized human glomerular mesangial cells in culture, with unique migratory properties, Am. J. Physiol. Renal Physiol. 301 (2011) F1131–1138.
[13] S.C. Satchell, C.H. Tasman, A. Singh, L. Ni, J. Geelen, C.J. von Ruhland, M.J. O'Hare, M.A. Saleem, L.P. van den Heuvel, P.W. Mathieson, Conditionally immortalized human glomerular endothelial cells expressing fenestrations in response to VEGF, Kidney Int. 69 (2006) 1633–1640.
[14] A.H. Rosendahl, C. Gundewar, K. Said, E. Karnevi, R. Andersson, Celecoxib synergizes human pancreatic ductal adenocarcinoma cells to sorafenib-induced growth inhibition, Pancreatology 12 (2012) 219–226.
[15] F.E. Froeling, C. Feig, C. Chelala, R. Dobson, C.E. Mein, D.A. Tuveson, H. Clevers, I.R. Hart, H.M. Kocher, Retinoic acid-induced pancreatic stellate cell quiescence reduces paracrine Wnt-beta-catenin signaling to slow tumor progression, Gastroenterology 141 (2011) 1486-1497.
[16] N. Kim, W. Yoo, J. Lee, H. Kim, H. Lee, Y.S. Kim, D.U. Kim, J. Oh, Formation of vitamin A lipid droplets in pancreatic stellate cells requires albumin, Gut 58 (2009) 1382–1390.
[17] M. Erkan, C. Reiser-Erkan, C.W. Michalski, S. Deucker, D. Sauliunaite, S. Streit, I. Esposito, H. Friess, J. Kleeff, Cancer-stellate cell interactions perpetuate the hypoxia-fibrosis cycle in pancreatic ductal adenocarcinoma, Neoplasia 11 (2009) 497–508.
[18] R. Hildenbrand, M. Niedergethmann, A. Marx, D. Belharazem, H. Allgayer, C. Schleger, P. Strobel, Amplification of the urokinase-type plasminogen activator receptor (uPAR) gene in ductal pancreatic carcinomas identifies a clinically high-risk group, Am. J. Pathol. 174 (2009) 2246–2253.
[19] E. Pardali, D.W. van der Schaft, E. Wiercinska, A. Gorter, P.C. Hogendoorn, A.W. Griffioen, P. ten Dijke, Critical role of endoglin in tumor cell plasticity of Ewing sarcoma and melanoma, Oncogene 30 (2011) 334–345.
[20] S.K. Meurer, M. Alsamman, H. Sahin, H.E. Wasmuth, T. Kisseleva, D.A. Brenner, C. Trautwein, R. Weiskirchen, D. Scholten, Overexpression of endoglin modulates TGF-beta1-signalling pathways in a novel immortalized mouse hepatic stellate cell line, PLoS One 8 (2013) e56116.
[21] H. Tian, K. Mythreye, C. Golzio, N. Katsanis, G.C. Blobe, Endoglin mediates fibronectin/alpha5beta1 integrin and TGF-beta pathway crosstalk in endothelial cells, Embo J. 31 (2012) 3885–3900.
[22] A. Masamune, M. Satoh, K. Kikuta, N. Suzuki, T. Shimosegawa, Endothelin-1 stimulates contraction and migration of rat pancreatic stellate cells, World J. Gastroenterol. 11 (2005) 6144–6151.
[23] S. Kondo, H. Ueno, H. Hosoi, J. Hashimoto, C. Morizane, F. Koizumi, K. Tamura, T. Okusaka, Clinical impact of pentraxin family expression on prognosis of pancreatic carcinoma, Br. J. Cancer 109 (2013) 739–746.
[24] M. Erkan, N. Weis, Z. Pan, C. Schwager, T. Samkharadze, X. Jiang, U. Wirkner, N.A. Giese, W. Ansorge, J. Debus, P.E. Huber, H. Friess, A. Abdollahi, J. Kleeff, Organ-, inflammation- and cancer specific transcriptional fingerprints of pancreatic and hepatic stellate cells, Mol. Cancer 9 (2010) 88.
[25] E.P. Kopantzev, E. Usova, M. Kopantseva, T. Azhikina, T. Skvortsov, O. Bychenko, M. Zinovyeva, M. Kostina, V. Egorov, A. Fedorov, and E.D. Sverdlov, Abstract 4277: Comparative gene expression analysis of proliferating stromal cells from pancreatic ductal adenocarcinoma, pancreatitis and normal pancreas. Proceedings: AACR 103rd Annual Meeting 2012, Cancer Res. **72**(8 Suppl), 2012, 4277.
[26] U. Bergmann, H. Funatomi, M. Yokoyama, H.G. Beger, M. Korc, Insulin-like growth factor I overexpression in human pancreatic cancer: evidence for autocrine and paracrine roles, Cancer Res. 55 (1995) 2007–2011.
[27] M. Pollak, The insulin and insulin-like growth factor receptor family in neoplasia: an update, Nat. Rev. Cancer 12 (2012) 159–169.
[28] S. Rohrmann, V.A. Grote, S. Becker, S. Rinaldi, A. Tjonneland, N. Roswall, H. Gronbaek, K. Overvad, M.C. Boutron-Ruault, F. Clavel-Chapelon, A. Racine, B. Teucher, H. Boeing, D. Drogan, V. Dilis, P. Lagiou, A. Trichopoulou, D. Palli, G. Tagliabue, R. Tumino, P. Vineis, A. Mattiello, L. Rodriguez, E.J. Duell, E. Molina-Montes, M. Dorronsoro, J.M. Huerta, E. Ardanaz, S. Jeurnink, P.H. Peeters, B. Lindkvist, D. Johansen, M. Sund, W. Ye, K.T. Khaw, N.J. Wareham, N.E. Allen, F.L. Crowe, V. Fedirko, M. Jenab, D.S. Michaud, T. Norat, E. Riboli, H.B. Bueno-de-Mesquita, R. Kaaks, Concentrations of IGF-I and IGFBP-3 and pancreatic cancer risk in the European prospective investigation into cancer and nutrition, Br. J. Cancer 106 (2012) 1004–1010.
[29] C.M. Perks, E.G. Vernon, A.H. Rosendahl, D. Tonge, J.M. Holly, IGF-II and IGFBP-2 differentially regulate PTEN in human breast cancer cells, Oncogene 26 (2007) 5966–5972.
[30] R. Novosyadlyy, J. Dudas, R. Pannem, G. Ramadori, J.G. Scharf, Crosstalk between PDGF and IGF-I receptors in rat liver myofibroblasts: implication for liver fibrogenesis, Lab Invest. 86 (2006) 710–723.
[31] J. Ma, H. Sawai, Y. Matsuo, N. Ochi, A. Yasuda, H. Takahashi, T. Wakasugi, H. Funahashi, M. Sato, H. Takeyama, IGF-1 mediates PTEN suppression and enhances cell invasion and proliferation via activation of the IGF-1/PI3K/Akt signaling pathway in pancreatic cancer cells, J. Surg. Res. 160 (2010) 90–101.
[32] Z. Xu, A. Vonlaufen, P.A. Phillips, E. Fiala-Beer, X. Zhang, L. Yang, A.V. Biankin, D. Goldstein, R.C. Pirola, J.S. Wilson, M.V. Apte, Role of pancreatic stellate cells in pancreatic cancer metastasis, Am. J. Pathol. 177 (2010) 2585–2596.
[33] D. Metalli, F. Lovat, F. Tripodi, M. Genua, S.Q. Xu, M. Spinelli, L. Alberghina, M. Vanoni, R. Baffa, L.G. Gomella, R.V. Iozzo, A. Morrione, The insulin-like growth factor receptor I promotes motility and invasion of bladder cancer cells through Akt- and mitogen-activated protein kinase-dependent activation of paxillin, Am. J. Pathol. 176 (2010) 2997–3006.
[34] A. Rosendahl, G. Forsberg, Influence of IGF-IR stimulation or blockade on proliferation of human renal cell carcinoma cell lines, Int. J. Oncol. 25 (2004) 1327–1336.